

# Relationship between Cr-Al Interaction and the Performance of Cr-Al<sub>2</sub>O<sub>3</sub> Catalysts for Isobutane Dehydrogenation

Deren Fang\*, Jinbo Zhao, Shang Liu, Limei Zhang, Wanzhong Ren, Huimin Zhang

Engineering Center of Petrochemical Light Hydrocarbon Comprehensive Utilization of Shandong Province, Yantai University, Yantai, China  
Email: \*[fdr@ytu.edu.cn](mailto:fdr@ytu.edu.cn)

Received 1 April 2015; accepted 21 April 2015; published 22 April 2015

Copyright © 2015 by authors and Scientific Research Publishing Inc.  
This work is licensed under the Creative Commons Attribution International License (CC BY).  
<http://creativecommons.org/licenses/by/4.0/>



Open Access

---

## Abstract

A series of catalysts were prepared using the kneading molding method and the impregnation method as well as the dry mix method by using different raw materials. By using X-ray diffraction (XRD), X-ray photoelectron spectroscopy (XPS), and temperature-programmed reduction (TPR) techniques, we studied the relationship between the catalyst performance and the Cr-Al interaction in the catalytic dehydrogenation of isobutane. The results demonstrated that the Cr-Al interaction in the catalyst had a direct influence on the catalytic activity and the selectivity of isobutene. The catalysts prepared using the kneading molding method had higher catalytic activity and isobutene selectivity than those prepared using the dry mix method. By comparison, XRD, XPS, and TPR results showed that the greater the Cr-Al interaction in the catalyst was, the higher the catalytic activity was. Here, we propose a mechanism of isobutane dehydrogenation.

## Keywords

Isobutane Dehydrogenation, Cr/Al<sub>2</sub>O<sub>3</sub>, Cr-Al Interaction, Catalyst, Mechanism

---

## 1. Introduction

Isobutylene is a major component of methyl tert butylether (MTBE) and methacrylate synthesis. Extensive research has been conducted on isobutylene synthesis by nonoxidative [1] [2] and oxidative [3]-[6] processes as well as steam cracking [7] [8]. Presently, isobutylene is produced industrially by the endothermic dehydrogenation of isobutene by using the Cr<sub>2</sub>O<sub>3</sub>-Al<sub>2</sub>O<sub>3</sub> catalyst at 900 K with a residence time of approximately 1 s. In this

\*Corresponding author.

process, the selectivity of the catalyst to isobutylene is more than 90% and the conversion of isobutane is 40% - 50% [1]. Higher temperatures favor coke formation, requiring frequent catalyst regeneration. Several studies have been performed using chromium catalysts [9]-[17] and have provided useful results. Although Al-Zahrani *et al.* [13] [16] suggested that the catalytic active center might be  $\text{Cr}^{3+}$ , they presented no direct evidence in support of this hypothesis. Recently, we studied the characteristics and deactivation of the catalytic active center of Cr- $\text{Al}_2\text{O}_3$  catalysts for isobutane dehydrogenation and demonstrated that the catalytic active center was  $\text{Cr}^{2+}/\text{Cr}^{3+}$ , produced from  $\text{Cr}^{6+}$  by the on-line reduction of hydrocarbon and carbon monoxide; the deactivation of Cr- $\text{Al}_2\text{O}_3$  was mainly caused by carbon deposition on the surface of the catalyst [18]. To date, the knowledge of the relationship between the Cr-Al interaction and the catalytic performance of chromium catalysts in isobutane dehydrogenation remains limited; thus, systematic research on this reaction is required.

By using X-ray diffraction (XRD), X-ray photoelectron spectroscopy (XPS), and temperature-programmed reduction (TPR) techniques, we studied the relationship between Cr-Al interaction and the performance of the Cr- $\text{Al}_2\text{O}_3$  catalyst as well as the nature of the catalytic active center. In this study, we obtained a considerable amount of valuable information on the relationship between catalyst performance and the Cr-Al interaction in the dehydrogenation of isobutane. Based on a literature search, this is the first report on the effect of Cr-Al interaction on the performance of catalysts in the dehydrogenation of isobutane.

## 2. Experimental

### 2.1. Sample Preparation

Chromium oxide catalysts, Cr- $\text{Al}_2\text{O}_3$ , were prepared using various methods. Two samples were prepared using the kneading molding method by using pseudoboehmite with chromic nitrate or chromic acetate as raw material, dried at 110°C and roasted at 600°C for 2 h, and designated as KN-1 and KN-2. Two samples were prepared using the impregnation method by using pseudoboehmite and by using a microballoon of  $\gamma\text{-Al}_2\text{O}_3$  with chromic nitrate or chromic acetate as raw material, dried at 110°C and roasted at 600°C for 2 h, and designated as IP-1 and IP-2. Three samples were prepared using the dry mix method by using powdered chromic hydroxide and pseudoboehmite as raw material. First, chromic hydroxide and pseudoboehmite were roasted at 600°C for 2 h. One sample was then prepared by physically mixing chromium hemitrioxide and aluminum oxide and was designated as CA-1. Another sample was prepared by physically mixing chromium hemitrioxide and aluminum oxide and roasted at 600°C for 2 h and was designated CA-2. Another sample was prepared by physically mixing powdered chromic hydroxide and pseudoboehmite and roasting them at 600°C for 2 h, designated as CA-3. All of the aforementioned catalysts had a similar final chemical composition with a weight percentage of 15% of chromium hemitrioxide. A sample containing pure chromium hemitrioxide was prepared by roasting chromic hydroxide at 600°C and was designated as CP-1. A sample containing pure aluminum oxide was obtained by roasting pseudoboehmite at 600°C and was designated as AP-1.

### 2.2. Sample Characterization

Powder XRD patterns of the solid products were studied using a Shimadzu XRD-6100 X-ray diffractometer (Cu K radiation) equipped with a computer system to perform automatic operation and data processing.

XPS was performed using a Thermo Fisher Scientific ESCALAB 250 spectrometer equipped with a standard Mg K-alpha source and a high performance Al monochromatic source. XPS spectra were referenced to the C1s peak at 284.6 eV.

The BET surface areas of the catalysts were measured through nitrogen adsorption by using an ASAP2010 type Quanta chrome NOVA automated gas sorption system.

TPR was performed using a TP5000 multifunction absorber equipped with a computer system to perform automatic operation and data recording. The effluent gas was passed through a dryer tube to remove water before detection. The catalyst weight was 20 mg and the particle size was 60 - 80 mesh. The inner diameter of the quartz reactor was 3 mm with a built-in thermocouple used to monitor the temperature. A mixture of 10%  $\text{H}_2$  and 90%  $\text{N}_2$  was used as the reduction gas and the rate of temperature increase was 10°C/min.

The dehydrogenation activity of Cr- $\text{Al}_2\text{O}_3$  catalysts for isobutene dehydrogenation was determined using a  $\Phi$  28 × 3 × 100-mm stainless steel reactor with an inner diameter of 22 mm. The bed height of the catalysts was 10 mm. Isobutane was introduced into the reactor from the bottom of the reactor. The reaction was performed at

atmospheric pressure and under isothermal conditions, with temperatures at  $600^{\circ}\text{C} \pm 5^{\circ}\text{C}$ . The effluent of the reaction was analyzed using gas chromatography on-line by using an FID detector and an  $\text{Al}_2\text{O}_3$  capillary column.

### 3. Results and Discussion

#### 3.1. Phase Characterization

The state of the catalysts prepared using the three methods is shown in **Figure 1(a)**, **Figure 1(b)**, and **Figure 1(c)**. Based on the XRD patterns, we observed that the major state of all the catalysts was amorphous  $\gamma\text{-Al}_2\text{O}_3$ , and in some catalysts, crystalline  $\text{Cr}_2\text{O}_3$  phase was observed. In CP-1, the main state of chromium hemitrioxide was  $\text{Cr}_2\text{O}_3$  (**Figure 1(a)**), the phase of  $\text{CrO}_3$  was not detected, which may be existed with the amorphous state and will be detected using XPS and TPR techniques. In AP-1, the main phase of aluminum trioxide was amorphous  $\gamma\text{-Al}_2\text{O}_3$ . In the CA-1, CA-2, and CA-3 samples (**Figure 1(b)**), some amount of  $\text{Cr}_2\text{O}_3$  was detected, and the amount of  $\text{Cr}_2\text{O}_3$  present decreased in the following order: CA-1 > CA-2 > CA-3. This finding indicates that the Cr-Al interaction increased in the following order: CA-1 < CA-2 < CA-3. We did not detect the presence of  $\text{Cr}_2\text{O}_3$  in the samples prepared using the kneading molding method; however, we detected a small amount of  $\text{Cr}_2\text{O}_3$  in the IP-2 sample formed using the impregnation method (**Figure 1(c)**). The results demonstrated that the contact of the chromium compound with aluminum oxide was more closely the interaction between Cr-Al was more strong to avoid the separate out of  $\text{Cr}_2\text{O}_3$  phase.

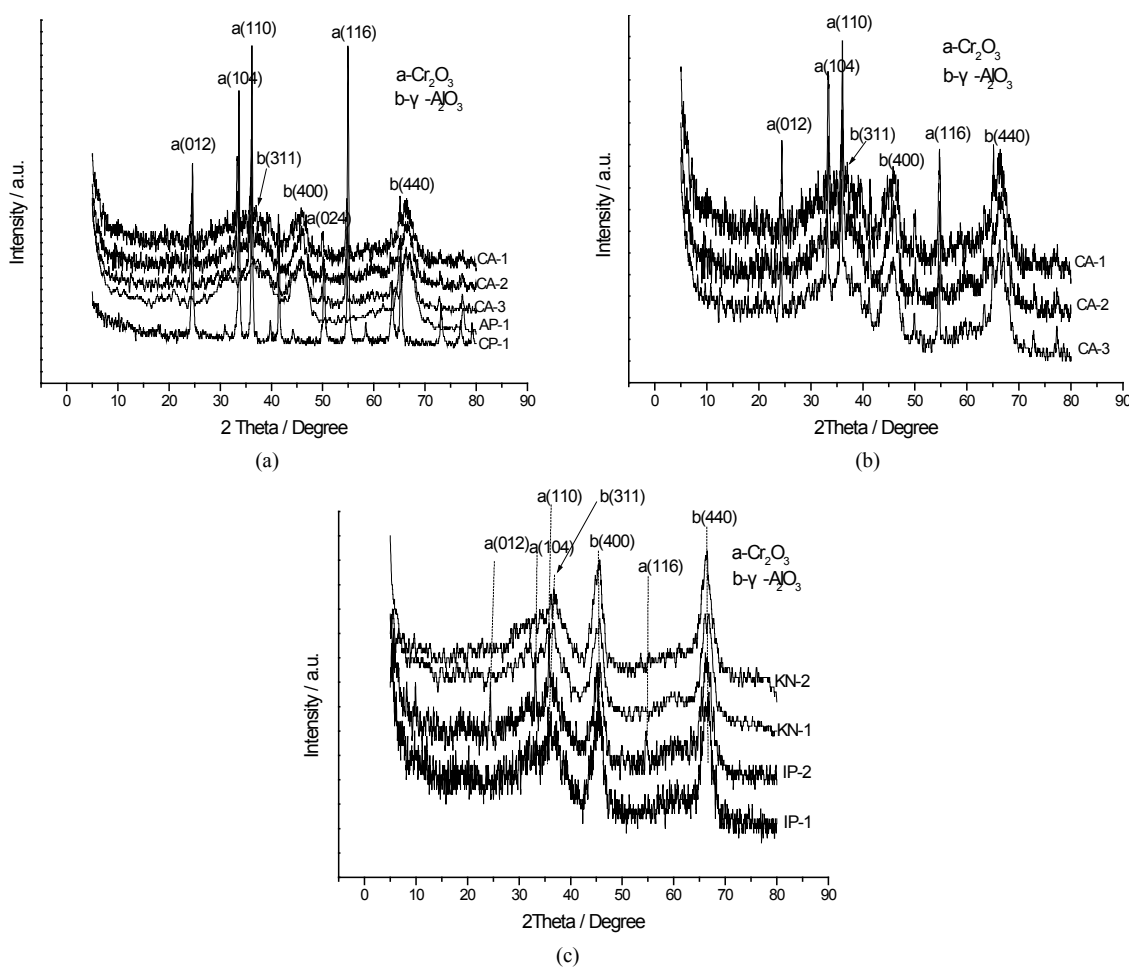


**Figure 1.** The XRD pattern of catalysts made by various methods. (a) Samples made by physically mixing method (CA-1, 2, 3) and pure materials (CP-1, AP-1); (b) Samples made by physically mixing method (CA-1, 2, 3); (c) Samples made by kneading molding method (KN-1, 2) and impregnation method (IP-1, 2).

The XPS spectra of Cr2p (**Figure 2**) demonstrated that in all of the catalysts, Cr2p<sub>3/2</sub> had two main peaks at 577.5 eV and 579.4 eV, which correspond to the binding energy of Cr<sup>3+</sup> and Cr<sup>6+</sup>, respectively [18]-[20]. For the sample containing pure chromium hemitrioxide (CP-1), Cr2p<sub>3/2</sub> had three peaks at 575.2 eV, 576.4 eV, and 579.3 eV. The first peak at 575.2 eV may represent the binding energy of Cr<sup>3+</sup>, and the binding energy of pure chromium hemitrioxide was lower in CP-1 than in other catalysts, indicating that the Cr-Al interaction affects the state of chromium. The XPS spectra of the samples prepared using the kneading molding and impregnation methods showed that the preparation method influenced the state of chromium (**Figure 2(b)**). The content of Cr<sup>6+</sup> in the samples KN-1 and KN-2 was more than that in the IP-1 and IP-2 samples, and the peak gradually shifted from 579.4 eV to 580.5 eV. In addition, while comparing the Cr2p XPS spectra of KN-1 with that of KN-2 and the Cr2p XPS spectra of IP-1 with that of IP-2, we observed that the raw material used for the preparation of different samples altered the state of chromium. The intensity of the second peak was stronger for the samples KN-1 and IP-1 than for the samples KN-2 and IP-2. This finding demonstrated that the Cr-Al interaction was stronger in KN-1 and IP-1. For the CA-1, CA-2, and CA-3 samples (**Figure 2(c)**), prepared by physically mixing different raw materials, the major state of chromium was Cr<sup>3+</sup> and some amount of Cr<sup>6+</sup>, and the amount of Cr<sup>6+</sup> increased in the following order: CA-1 < CA-2 < CA-3. This result revealed that the preparation method and raw materials have a considerable effect on the state of chromium.

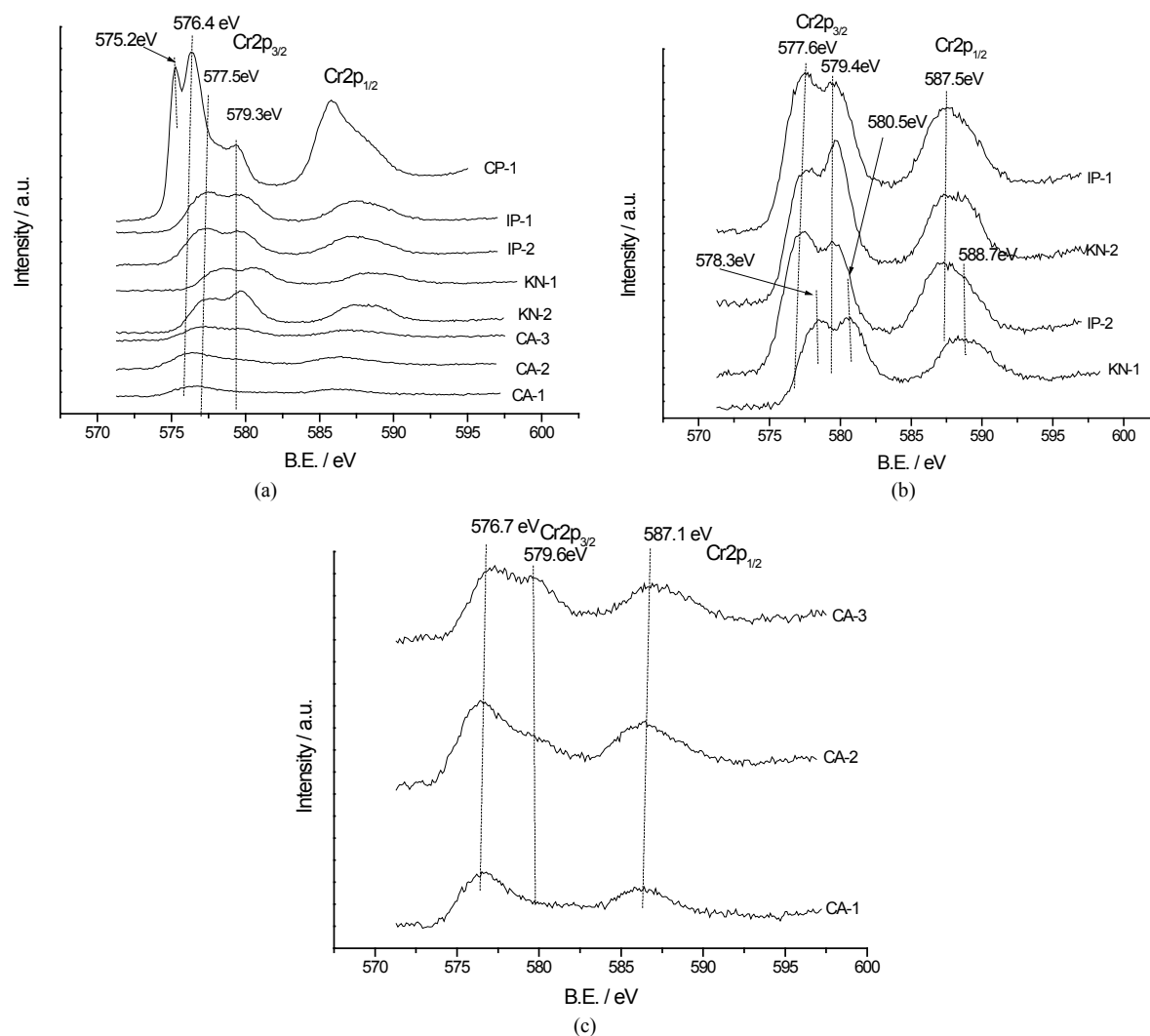


**Figure 2.** XPS spectra for Cr2p of catalysts made by various methods. (a) Samples made by physically mixing method (CA-1, 2, 3) and pure materials (CP-1, AP-1); (b) Samples made by physically mixing method (CA-1, 2, 3); (c) Samples made by kneading molding method (KN-1, 2) and impregnation method (IP-1, 2).

The XPS spectra of Al2p (**Figure 3**) for the CA-1, CA-2, and CA-3 samples revealed that the binding energy gradually shifted from 74.4 eV to 75.0 eV; this result was consistent with that of Cr2p. The samples prepared using the kneading molding and impregnation methods showed differences in the binding energy and the peak gradually shifted from 77.5 eV to 79.6 eV in the following order: IP-2 < IP-1 < KN-2 < KN-1. For example, the peak of KN-1 shifted to 79.6 eV. Thus, the Cr-Al interaction altered the state of both chromium and aluminum; these results were consistent with those of our previous study [18].

### 3.2. TPR Results

TPR was performed to determine the state of chromium. The TPR curve of the catalysts is shown in **Figure 4**. The samples prepared using the kneading molding and impregnation methods showed a single reduction peak at approximately 360°C - 370°C; this result was consistent with that of our previous study, in which the reduction peak of Cr<sup>6+</sup> to Cr<sup>3+</sup> was at approximately 360°C - 370°C [18]. For the sample containing pure chromium hemi-trioxide (CP-1), the TPR curve demonstrated two reduction peaks at 320°C and 410°C. According to the results of our previous study, because Cr<sup>3+</sup> cannot be reduced by hydrogen, both reduction peaks must have been

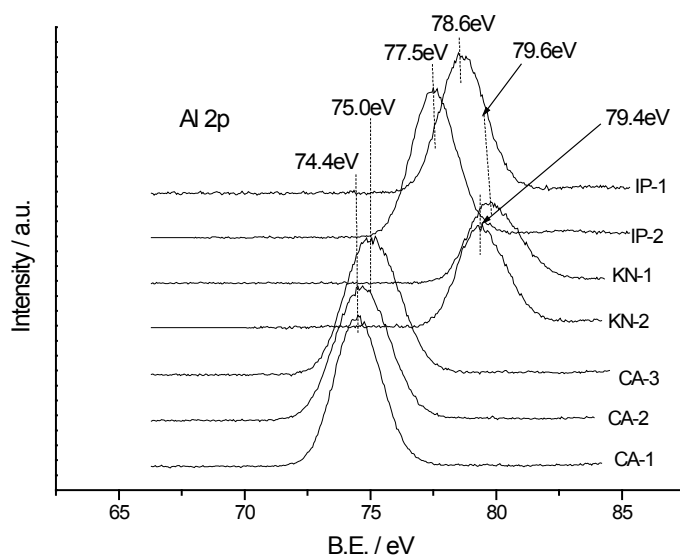


**Figure 3.** XPS spectra for Al2p of catalysts made by various methods.

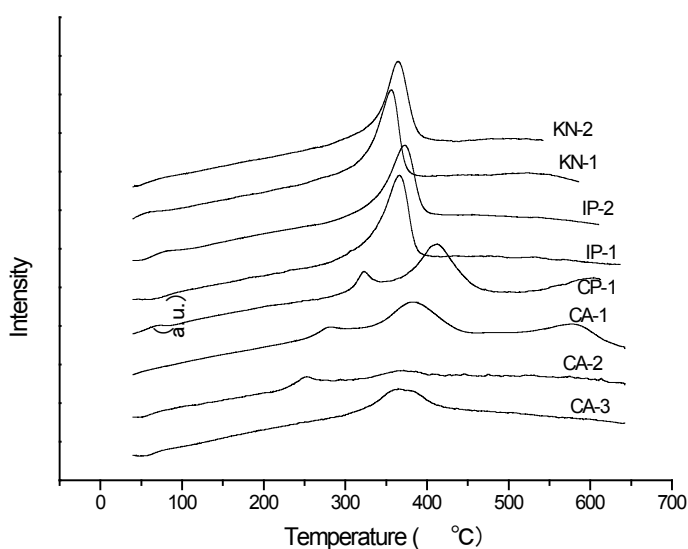


**Figure 4.** TPR curve for catalysts made by various methods.

caused by the reduction of  $\text{Cr}^{6+}$  to  $\text{Cr}^{3+}$  [18], which may be attributable to the reduction of free-form  $\text{CrO}_3$  and bulk  $\text{CrO}_3$ . For the CA-1 and CA-2 samples, two reduction peaks were observed at  $280^\circ\text{C}$  and  $380^\circ\text{C}$  for CA-1 and at  $250^\circ\text{C}$  and  $360^\circ\text{C}$  for CA-2, and the intensity decreased as follows:  $\text{CP-1} > \text{CA-1} > \text{CA-2}$ . For the CA-3 sample, a single reduction peak was observed at  $370^\circ\text{C}$ . These results suggest that in the aforementioned catalysts,  $\text{CrO}_3$  was dispersed on the surface of the catalyst and had some interaction with the bulk phase of the catalysts, which effect of strength is lower than the bulk phase of  $\text{CrO}_3$  but higher than the free form surface  $\text{CrO}_3$ . When comparing the peak intensity of KN-1, KN-2, IP-1, and IP-2 with that of CA-1, CA-2, and CA-3, we discovered that the content of  $\text{CrO}_3$  was considerably higher in KN-1, KN-2, IP-1, and IP-2 than in CA-1, CA-2, and CA-3. The contact surface for CA-1, CA-2, and CA-3 was considerably more than that for KN-1, KN-2, IP-1, and IP-2 because the chromium salts in CA-1, CA-2, and CA-3 existed in molecular form in the solution. Thus, the contact surface had the most effect on the dispersion of  $\text{CrO}_x$  species on the catalyst and the Cr-Al interaction. TPR results demonstrated that all the samples contained  $\text{CrO}_3$ , and these results were consistent with the XPS results, and their amounts increased as the Cr-Al interaction increased. The XPS and TPR results revealed that the method of preparation of the catalysts altered the dispersion of  $\text{CrO}_x$  species on the catalysts and the Cr-Al interaction in the catalysts.

### 3.3. Physical Parameters of Catalysts

The physical parameters of the catalysts are shown in **Figure 5** and **Table 1**. **Figure 5** shows that the preparation method and raw materials have a substantial effect on the pore distribution of catalysts. The catalysts prepared using the kneading molding method had a smaller pore size and a smaller surface area (**Table 1**) than those prepared using other methods. Regarding the raw materials, chromic nitrate facilitates the formation of large pores. The sample containing pure chromium hemitrioxide (CP-1) had an extremely lower surface area and pore volume than other catalysts; in other words, the addition of aluminum results in a large surface area. The samples prepared by physically mixing chromium hemitrioxide and aluminum oxide and by using the impregnation method had similar surface area and pore size, indicating that aluminum primarily determined the physical parameters of the catalysts.

### 3.4. Catalytic Activity

The reaction results are shown in **Table 2**.

**Table 2** shows the conversion of isobutane and the product selectivity of the  $\text{Cr-Al}_2\text{O}_3$  catalysts. The results clearly show that the conversion of isobutane and the selectivity of isobutene increased in the following order:  $\text{CP-1} < \text{CA-1} < \text{CA-2} < \text{CA-3} < \text{IP-2} < \text{IP-1} < \text{KN-2} < \text{KN-1}$ . Specifically, the stronger the Cr-Al interaction, the higher the conversion and the selectivity of isobutene. For the sample containing pure chromium hemitrioxide

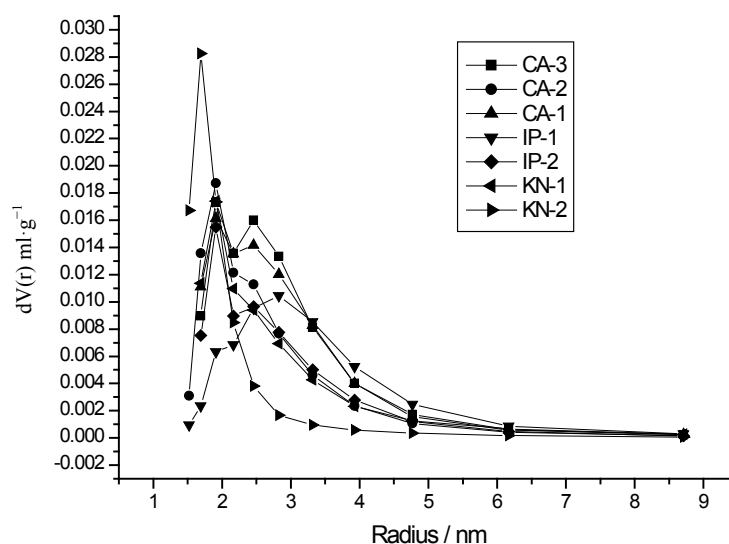


**Figure 5.** Pore distribution curves of catalysts.

**Table 1.** The specific surface area and porosity of catalysts.

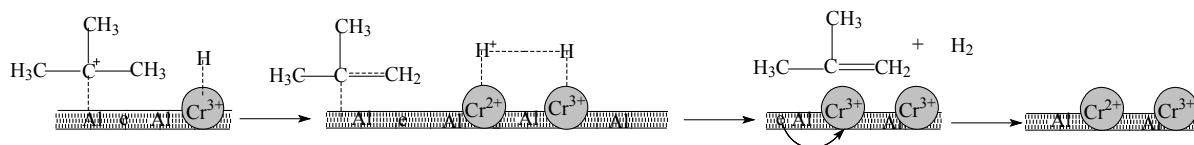
Sample	CP-1	CA-1	CA-2	CA-3	KN-1	KN-2	IP-1	IP-2
Surface area /m <sup>2</sup> ·g <sup>-1</sup>	14.28	167.1	150.2	173.7	152.8	149.7	121.9	120.4
Pore radius /nm	8.83	1.93	1.93	1.91	1.92	1.93	2.83	1.91
Pore volume/ml·g <sup>-1</sup>	0.058	0.303	0.247	0.321	0.229	0.223	0.255	0.213

**Table 2.** The catalytic activity and selectivity of products of the Cr-Al<sub>2</sub>O<sub>3</sub> catalysts.

Sample	Conversion of isobutane/%		Selectivity of isobutene/%		Selectivity of methane/%		Selectivity of propane/%		Selectivity of propylene/%		Selectivity of n-butane/%		Selectivity of n-butene/%	
	550°C	600°C	550°C	600°C	550°C	600°C	550°C	600°C	550°C	600°C	550°C	600°C	550°C	600°C
CP-1	4.78	8.80	6.77	32.0	2.63	3.67	11.6	7.56	1.50	10.5	70.5	45.5	2.10	1.50
AP-1*	6.51	13.1	15.7	28.9	2.73	5.42	6.75	5.71	7.25	8.73	12.9	13.2	4.75	8.75
CA-1	7.76	16.7	21.6	36.2	1.98	8.85	10.8	6.69	4.99	16.5	52.1	22.9	3.56	6.56
CA-2	16.5	25.5	80.6	72.2	1.20	3.67	5.01	6.40	2.27	5.83	4.99	1.72	1.10	2.51
CA-3	21.2	30.8	84.2	75.8	1.33	3.80	4.32	5.50	2.10	5.22	3.50	1.75	1.32	1.95
IP-1	29.9	41.9	91.0	84.1	1.50	2.56	1.72	3.65	1.35	3.96	0.85	0.76	0.45	0.51
IP-2	23.0	38.9	89.6	80.9	1.50	5.10	2.60	4.73	1.51	5.53	0.73	0.50	0.50	0.39
KN-1	35.9	47.7	94.1	87.0	0.40	2.80	1.10	3.42	0.61	6.45	0.56	0.25	0.51	0.40
KN-2	31.7	43.3	92.2	85.1	1.62	4.52	2.35	4.53	1.45	6.10	0.88	0.77	0.55	0.56

\*AP-1 does not contain the liquid products.

(CP-1), both the catalytic activity and the selectivity of isobutene were lower, and had higher selectivity for n-butane. The results also demonstrated that pure Cr<sub>2</sub>O<sub>3</sub> had a far lower catalytic activity for isobutane dehydrogenation in the temperature range of 550°C - 600°C. The sample containing pure aluminum oxide (AP-1) had a higher catalytic activity than that of the sample containing pure chromium hemitrioxide (CP-1); however, several byproducts, such as liquid hydrocarbon (not shown in **Table 1**), were produced when using the sample containing pure aluminum oxide. Thus, polymerization occurred when using the sample containing pure aluminum oxide. Both the samples containing pure chromium hemitrioxide (CP-1) or pure aluminum oxide (AP-1) had lower isobutene selectivity. After comparing the results of CA-1, CA-2, and CA-3, we discovered that in CA-3, the sample prepared by roasting the mixture of chromic hydroxide and pseudoboehmite, the activity and selectivity increased because the raw materials could react during roasting and produce more catalytic activity centers. Regarding CA-1, the sample prepared by physically mixing Cr<sub>2</sub>O<sub>3</sub> and Al<sub>2</sub>O<sub>3</sub>, the catalyst had a smaller activity center because the interaction between Cr<sub>2</sub>O<sub>3</sub> and Al<sub>2</sub>O<sub>3</sub> particles was not as intimate as that in CA-2 and CA-3. Regarding CA-2, the catalytic activity and selectivity were between those of CA-1 and CA-3. This finding demonstrated that, for preparing catalysts CA-1 and CA-2, the raw materials were roasted before mixing, but interaction occurred between Cr and Al in the CA-2 catalyst after the second roasting process; in other words, Cr<sub>2</sub>O<sub>3</sub> and Al<sub>2</sub>O<sub>3</sub> particles can interact at 600°C in an air atmosphere. Compared with CA-2, the reduction of CA-1 reduced the Cr-Al interaction; in other words, chromium in the lower valence state did not easily react with Al<sub>2</sub>O<sub>3</sub> particles in the reduction atmosphere. After comparing the KN-1 sample with KN-2 or the IP-1 sample with IP-2, we discovered that catalysts prepared using chromic nitrate as the raw material had a higher catalytic activity and isobutene selectivity than those prepared using chromic acetate as the raw material. This result revealed that the Cr-Al interaction was greater in the catalysts prepared using chromic nitrate as the raw material than in the catalysts prepared using chromic acetate as the raw material. Because our previous study results demonstrated that the catalytic activity center may be Cr<sup>2+</sup>/Cr<sup>3+</sup> [18], the aforementioned results demonstrated that using chromic nitrate as the raw material is beneficial for the formation of catalytic centers. The CrO<sub>x</sub> species easily dispersed on the surface of aluminum oxide particles and reacted to form the special structure of a Cr-Al solid solution [21],



**Scheme 1.** Diagrammatic sketch of reaction mechanism of dehydrogenation of isobutene.

which became an active center in the reduction atmosphere. When we compared KN-1 with IP-1 and KN-2 with IP-2, we found that the method of catalyst preparation had a greater influence on the catalytic activity and isobutene selectivity. Regarding the samples prepared using the kneading molding method, the catalysts had a higher catalytic activity and selectivity than the samples prepared using the impregnation method, demonstrating that the use of aluminum as the raw material has a greater effect on the performance of the catalysts. In the kneading molding method, the combination of pseudoboehmite with chromic nitrate or chromic acetate had a higher reaction activity than the combination of aluminum with chromic nitrate or chromic acetate used in the impregnation method. In the impregnation method, aluminum oxide was roasted at 600°C before being mixed with chromic nitrate or chromic acetate and had a lower reaction activity than that of pseudoboehmite. The results of Chou, s demonstrated that the high conversion rate of isobutene was caused by its highly dispersed chromium species, whereas the high selectivity of isobutene was caused by the formation of chromia-alumina solid solutions in the catalysts [21]. Our aforementioned results suggested that the close interaction of  $\text{CrO}_x$  species with aluminum oxide is crucial to the dehydrogenation of isobutane; the catalytic active center has a close relationship with the Cr-Al interaction. Considering the aforementioned results, we speculate that the reaction mechanism of dehydrogenation of isobutane may be the result of the synergistic effect of  $\text{CrO}_x$  species with aluminum oxide, which can be illustrated as follows (**Scheme 1**). The reaction mechanism was that isobutane was first adsorbed on the Al surface and produced a carbonium ion and adsorbed a hydrogen atom on the  $\text{Cr}^{3+}$  site simultaneously. The carbonium ion then reacted with the  $\text{Cr}^{2+}$  site to produce isobutene adsorbed on the  $\text{Al}^{n+}$  site and a hydrogen ion adsorbed on the  $\text{Cr}^{2+}$  site, which then combined with the adsorbed hydrogen atom on the  $\text{Cr}^{3+}$  site to form molecular hydrogen, while the  $\text{Cr}^{2+}$  site was oxidized to  $\text{Cr}^{3+}$ , which was reduced by hydrocarbons or carbon monoxide to  $\text{Cr}^{2+}$  species, as we previously reported [18].

## 4. Conclusion

We prepared Cr- $\text{Al}_2\text{O}_3$  catalysts for the dehydrogenation of isobutene by using different methods. The properties of these catalysts were studied using various techniques and considerable information was obtained. Our results demonstrated that both the preparation method and raw materials had a considerable effect on the properties of the catalysts. The catalysts prepared using the kneading molding method and with chromic nitrate and pseudoboehmite as raw materials had the highest catalytic activity and isobutene selectivity, whereas those prepared by physically mixing raw materials had the lowest catalytic activity and isobutene selectivity. The preparation method and raw materials mainly altered the Cr-Al interaction, which, in turn, influenced the performance of the catalysts. The close interaction of  $\text{CrO}_x$  species with aluminum oxide is crucial to the dehydrogenation of isobutane; in other words, the catalytic active center has a close relationship with the Cr-Al interaction. The dehydrogenation of isobutane on Cr/ $\text{Al}_2\text{O}_3$  catalysts may be caused by the synergistic effect of  $\text{Al}^{n+}$ - $\text{Cr}^{2+}$ / $\text{Cr}^{3+}$ .

## Acknowledgements

This work is supported by the Natural Science Foundation of ShanDong Province of China (ZR2013BM008).

## References

- [1] Matsuda, T., Koike, I., Kubo, N. and Kikuchi, E. (1993) Dehydrogenation of Isobutane to Isobutene in a Palladium Membrane Reactor. *Applied Catalysis A*, **96**, 3-13.
- [2] de Rossi, S., Ferraris, G., Freminotti, S., Indovina, V. and Cimino, A. (1993) Isobutane Dehydrogenation on Chromia/Zirconia Catalysts. *Applied Catalysis A*, **106**, 125-141.
- [3] Fontfreide, J.J.H.M., Howard, M.J. and Lomas, T.A. (1989) EP Patent 0 332 289 A2.
- [4] Al-Zahrani, S.M., Elbashir, N.O., Abasaed, A.E. and Abdulwahed, M. (2000) Oxidative Dehydrogenation of Isobu-

- tane over Pyrophosphates Catalytic Systems. *Catalysis Letters*, **69**, 65-70.
- [5] Mamedov, E.A. and Corberan, V.C. (1995) Oxidative Dehydrogenation of Lower Alkanes on Vanadium Oxide-Based Catalysts. The Present State of the Art and Outlooks. *Applied Catalysis A*, **127**, 1-40.
- [6] Harrison, P.G. and Argent, A. (1986) EP Patent 189 282 A1.
- [7] Yaluris, G., Rekoske, J.E., Aparicio, L.M., Madon, R.J. and Dumesic, J.A. (1995) Isobutane Cracking over Y-Zeolites: I. Development of a Kinetic-Model. *Journal of Catalysis*, **153**, 54-64. <http://dx.doi.org/10.1006/jcat.1995.1107>
- [8] Mirzabekova, S.R. and Mamedov, A.Kh. (1995) Oxidation of Hydrocarbons and Alcohols by Carbon Dioxide on Oxide Catalysts. *Industrial & Engineering Chemistry Research*, **34**, 474-482. <http://dx.doi.org/10.1021/ie00041a007>
- [9] Grabowski, R., Grzybowska, B., Stoczyfiski, J. and Wcisto, K. (1996) Oxidative Dehydrogenation of Isobutane on Supported Chromia Catalysts. *Applied Catalysis A*, **144**, 335-341.
- [10] Iannazzo, V., Neri, G., Galvagno, S., Serio, M.D., Tesser, R. and Santacesaria, E. (2003) Oxidative Dehydrogenation of Isobutane over V<sub>2</sub>O<sub>5</sub>-Based Catalysts Prepared by Grafting Vanadyl Alkoxides on TiO<sub>2</sub>-SiO<sub>2</sub> Supports. *Applied Catalysis A*, **246**, 49-68.
- [11] Moriceau, P., Grzybowska, B., Gengembre, L. and Barbaux, Y. (2000) Oxidative Dehydrogenation of Isobutane on Cr-Ce-O Oxide II: Physical Characterizations and Determination of the Chromium Active Species. *Applied Catalysis A*, **199**, 73-82.
- [12] Moriceau, P., Grzybowska, B., Barbaux, Y., Wrobel, G. and Hecquet, G. (1998) Oxidative Dehydrogenation of Isobutane on Cr-Ce-O Oxide: I. Effect of the Preparation Method and of the Cr Content. *Applied Catalysis A*, **68**, 269-277.
- [13] Al-Zahrani, S.M., Elbashir, N.O., Abasaeed, A.E. and Abdulwahed, M. (2001) Catalytic Performance of Chromium Oxide Supported on Al<sub>2</sub>O<sub>3</sub> in Oxidative Dehydrogenation of Isobutane to Isobutene. *Industrial & Engineering Chemistry Research*, **40**, 781-784. <http://dx.doi.org/10.1021/ie000334x>
- [14] Karamullaoglu, G., Onen, S. and Dogu, T. (2002) Oxidative Dehydrogenation of Ethane and Isobutane with Chromium-Vanadium-Niobium Mixed Oxide Catalysts. *Chemical Engineering and Processing*, **41**, 337-347. [http://dx.doi.org/10.1016/S0255-2701\(01\)00150-7](http://dx.doi.org/10.1016/S0255-2701(01)00150-7)
- [15] Elbashir, N.O., Al-Zahrani, S.M., Abasaeed, A.E. and Abdulwahed, M. (2003) Alumina-Supported Chromium-Based Mixed-Oxide Catalysts in Oxidative Dehydrogenation of Isobutane to Isobutene. *Chemical Engineering and Processing*, **42**, 817-823. [http://dx.doi.org/10.1016/S0255-2701\(02\)00108-3](http://dx.doi.org/10.1016/S0255-2701(02)00108-3)
- [16] Airaksinen, S.M.K., Harlin, M.E. and Krause, A.O.I. (2002) Kinetic Modeling of Dehydrogenation of Isobutane on Chromia/Alumina Catalyst. *Industrial & Engineering Chemistry Research*, **41**, 5619-5626. <http://dx.doi.org/10.1021/ie020371j>
- [17] Pinard, L., Bichon, P., Popov, A., Lemberton, J.L., Canaff, C., Mauge, F., *et al.* (2011) Identification of the Carbonaceous Compounds Present on a Deactivated Cobalt Based Fischer-Tropsch Catalyst Resistant to "Rejuvenation Treatment". *Applied Catalysis A*, **406**, 73-80.
- [18] Fang, D.R., Zhao, J.B., Li, W.J., Fang, X., Yang, X., Ren, W.Z. and Zhang, H.M. (2015) Investigation of the Characteristics and Deactivation of Catalytic Active Center of Cr-Al<sub>2</sub>O<sub>3</sub> Catalysts for Isobutane Dehydrogenation. *Journal of Energy Chemistry*, **24**, 101-107. [http://dx.doi.org/10.1016/S2095-4956\(15\)60290-X](http://dx.doi.org/10.1016/S2095-4956(15)60290-X)
- [19] Wang, S.B., Murata, K., Hayakawa, T., Hamakawa, S. and Suzuki, K. (2000) Dehydrogenation of Ethane with Carbon Dioxide over Supported Chromium Oxide Catalysts. *Applied Catalysis A*, **196**, 1-8.
- [20] Deng, S., Li, H.Q. and Zhang, Y. (2003) Oxidative Dehydrogenation of Ethane with Carbon Dioxide to Ethylene over Nanosized Cr<sub>2</sub>O<sub>3</sub> Catalysts. *Chinese Journal of Catalysis*, **24**, 744-750.
- [21] Zhao, H.H., Song, H.L., Miao, Z.C. and Chou, L.J. (2014) Isobutane Dehydrogenation over Chromia Alumina Catalysts Prepared from MIL-101: Insight into Chromium Species on Activity and Selectivity. *Journal of Energy Chemistry*, **23**, 708-716. [http://dx.doi.org/10.1016/S2095-4956\(14\)60203-5](http://dx.doi.org/10.1016/S2095-4956(14)60203-5)